Primljen / Received: 20.3.2017.
Ispravljen / Corrected: 10.10.2018.
Prihvaćen / Accepted: 15.11.2018.
Dostupno online / Available online: 10.7.2020.

Comparison of GFRP and CFRP confinement of normal and high strength concrete

Authors:

Muhammad Rameez Sohail, MSc. CE
rameez.sohail@uettaxila.edu.pk
Corresponding author

Assist.Prof. **Naveed Ahmad**, PhD. CE
naveed.ahmad@uettaxila.edu.pk

Muhammad Usman Rashid, MSc. CE
usman.rashid@uettaxila.edu.pk

Rana Waqas, MSc. CE
rana.waqas@uettaxila.edu.pk

Usman Muhammad, MSc. CE
usman.m@uettaxila.edu.pk

University of Engineering and Technology Taxila, Pakistan

Original scientific paper

Muhammad Rameez Sohail, Naveed Ahmad, Muhammad Usman Rashid, Rana Waqas, Usman Muhammad

Comparison of GFRP and CFRP confinement of normal and high strength concrete

An experimental and analytical study was conducted to quantify the increase in strength and ductility of GFRP and CFRP confined concrete cylinders made of normal strength concrete and high strength concrete. The test data are also compared with theoretical predictions from three North American and European FRP design guidelines. The test results show that the effectiveness of both GFRP and CFRP is more pronounced in normal strength concrete compared to high strength concrete.

Key words:
confinement of concrete, carbon fibres, glass fibres, longitudinal strain, volumetric strain, energy absorption

Izvorni znanstveni rad

Muhammad Rameez Sohail, Naveed Ahmad, Muhammad Usman Rashid, Rana Waqas, Usman Muhammad

Usporedba ovijanja betona normalne i visoke čvrstoće GFRP-om i CFRP-om

Provedeno je eksperimentalno i analitičko istraživanje kako bi se utvrdilo povećanje čvrstoće i duktilnosti betonskih uzoraka ovijenih GFRP-om i CFRP-om od betona normalne čvrstoće i betona visoke čvrstoće. Podaci ispitivanja uspoređeni su i s teorijskim predviđanjima iz triju sjevernoameričkih smjernica za izvedbu i europskih smjernica za FRP. Rezultati ispitivanja pokazuju kako je učinkovitost i GFRP-a i CFRP-a izraženija u betonu normalne čvrstoće u usporedbi s betonom visoke čvrstoće.

Ključne riječi:
ovijanje betona, ugljična vlakna, staklena vlakna, uzdužna deformacija, volumetrijska deformacija, apsorpcija energije

Wissenschaftlicher Originalbeitrag

Muhammad Rameez Sohail, Naveed Ahmad, Muhammad Usman Rashid, Rana Waqas, Usman Muhammad

Vergleich von normalen und hochfesten Betonhüllen mit GFK und CFK

Durchgeführt wurde eine experimentelle und analytische Untersuchung, um die Erhöhung der Festigkeit und Duktilität von GFK und CFK beschichteten Betonproben aus normalfestem Beton und hochfestem Beton festzustellen. Die Untersuchungsdaten wurden auch mit den theoretischen Vorhersagen aus den drei nordamerikanischen Richtlinien für die Ausführung und der europäischen FRP-Richtlinien verglichen. Die Ergebnisse der Untersuchungen zeigen, dass die Wirksamkeit sowohl von GFK also auch von CFK bei normalfestem Beton im Vergleich zu hochfestem Beton ausgeprägter ist.

Schlüsselwörter:
Betonhülle, Kohlefaser, Glasfaser, Längsverformung, Volumenverformung, Energieabsorption

1. Introduction

Structures currently in use are being subjected to increased service loads and severe environmental conditions. The rehabilitation and retrofitting of existing structures is traditionally done using steel or reinforced-concrete jacketing. But the relatively newer materials like fibre reinforced polymers are gaining in popularity because their properties are superior to those of conventional materials. Structural members reinforced with these materials have high strength to weight ratio, high corrosion resistance, longer life span, and enhanced ductility. Reinforced-concrete (RC) columns are critical members in a structure that resist vertical and lateral loads and are hence more vulnerable to failure during earthquakes [1]. Therefore, they must be retrofitted seismically, as has become clear after the collapse and damage of several RC structures during earthquakes. During an earthquake, good energy dissipation is facilitated by well-confined concrete resulting in structural safety. Structural fire is another hazard resulting in the deterioration of concrete strength [2] that can be retrofitted by FRP. Both normal strength concrete (NSC) and high strength concrete (HSC) exhibit different behaviour under fire conditions [3] and so an appropriate retrofit system should carefully be selected to meet strength requirements of such structures. This can be accomplished by selecting a suitable fibre reinforced polymer (FRP) confinement for structural concrete members susceptible to fire.

External wrapping of concrete structures using FRP composites provides a significant amount of lateral confinement leading to an increased axial strength and energy absorption as reported in literature [4-7]. Researchers have used several parameters like unconfined concrete strength, shape of specimens, presence of internal reinforcement, types of FRP, fibre orientations of FRP wraps, and number of confining FRP layers [8-13].

The stress-strain response of FRP confined concrete specimens is illustrated in Figure 1, as indicated in various above mentioned studies. It can be seen that the stress-strain response presented by Rahai et al. [8] is significantly stiffer compared to others, which can be attributed to the Carbon Fibre Reinforced Polymer (CFRP) confined high strength concrete having strength of 45 MPa. Pessiki et al [11] used cylindrical specimens 610 mm in height and 152 mm in diameter having internal reinforcement and FRP confinement, with fibre oriented at 45° with regard to hoop direction, which increased the ductility of specimens. This behaviour closely matches that of square unreinforced specimens tested by Rochette and Labossiere [12], which were wrapped with confining carbon fibres oriented at 15° with respect to hoop direction. This indicates that the behaviour of FRP confined concrete depends on the presence of internal reinforcement as well as on the shape of the specimen.

The confinement of circular concrete specimens 305 mm in height and 152.5 mm in diameter, tested by Parwin and Jamwal [10], shows quite a different response when compared to the results obtained by Mirmiran and Shahaway [5]. This is attributed to the number of layers used for confinement and their orientation, as well as to the type of confining material. It can be seen that with a smaller wrap thickness of the Glass Fibre Reinforced Polymer (GFRP), Parwin and Jamwal (2006) obtained stiffer stress-strain response, compared to the highly ductile response of 6, 10, and 14 plies of GFRP confinement used by Mirmiran and Shahaway

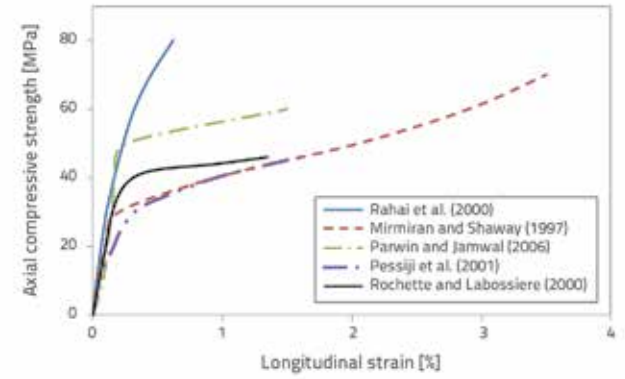

Figure 1. Stress-strain responses of various confined specimens.

The difference in the stress-strain response of FRP confined concrete can be attributed to the unconfined concrete strength, internal reinforcement, FRP (fibre) orientation of confinement, type of FRP used for confinement, and shape of the specimen. With such variation in parameters affecting behaviour of confined concrete, an accurate prediction of stress-strain response is quite difficult. Moreover, there is a need to validate the predictions by various design models and codes, as design is significantly affected by a number of variable parameters, as mentioned above. It is therefore desired to recognize and quantify a more effective and predictable confinement by studying the stress-strain response of two types of FRP systems, namely CFRP and GRRP.

2. Sample testing program and procedure

To study the comparative stress-strain response of GFRP and CFRP specimens, a comprehensive test program was conducted for 3 different strength concrete batches. The data obtained from tests was utilized to compare confinement characteristics provided by two types of FRPs. Moreover, the data was utilized to study and validate confinement predictions provided by different codes and guidelines.

2.1. Mix proportions and test specimens

A total of 27 cylinder specimens measuring 150 mm x 300 mm were cast in 3 batches of normal, medium, and high strength concrete. The mix proportions of these concrete batches are given in Table 1. The specimens were immersed in water and cured in water tank for 28 days. The wet lay-up method of FRP wrapping was employed. Out of 27 specimens, 9 were wrapped with carbon fibre reinforced polymer Sikawrap Hex 230C, and 9 specimens were wrapped with 2 wraps of glass fibre reinforced polymer Sikawrap Hex 106G, with the Sikadur 330 adhesive epoxy featuring a tensile strength

of 33.8 MPa and an elongation of 1.2% at breaking. The strength and physical properties of these materials are given in Table 2. The overlapping was kept at 10 cm according to the requirements of the system so as to avoid localized bond failure at overlap.

Table 1. Mix proportions

Ingredients	Series 1	Series 2	Series 3
Cement [kg/m³]	475	572	1071
Sand [kg/m³]	617	550	535
Aggregate [kg/m³]	1236	1144	1060
Water/cement ratio	0.4	0.4	0.35
BASF 850 [kg/m³]	0.171	-	-
SiO_2 [kg/m³]	-	1.38	2.21
FOSPAK 430R [kg/m³]	-	0.345	0.552
28 days compressive strength [MPa]	29.7	42.48	64.67

Table 2. Cured laminate properties of Sikawrap Hex 230C and Sikawrap Hex 106G with (Sikadur 330) epoxy

Property	Sikawrap Hex 230C	Sikawrap Hex 106G
Tensile strength [MPa]	715	244
Tensile elongation [%]	1.09	1.43
Tensile modulus [MPa]	59896	16215
Ply thickness [mm]	0.381	0.33

2.2. Test apparatus and procedure

The universal compression testing machine with a loading capacity of 2000 kN was utilized for axial compressive testing of the specimens. The Micro-Measurements P3 Strain Indicator and Recorder manufactured by Vishay Precision Group was used for strain measurements. This system is capable of recording strains through linear strain gauges using 4 input channels. The Vishay Micro-Measurements C2A-Series 062LW strain gauges with the resistance of 350 ohms were utilized for strain measurements. The strain gauges were attached to the specimens in horizontal, vertical and diagonal (45°) arrangement in order to measure longitudinal and lateral strains. Dial-type strain gauges were also used in every third test to cross check measurement accuracy of linear strain gauges. The test equipment, assembly, and arrangement are shown in Figure 2.

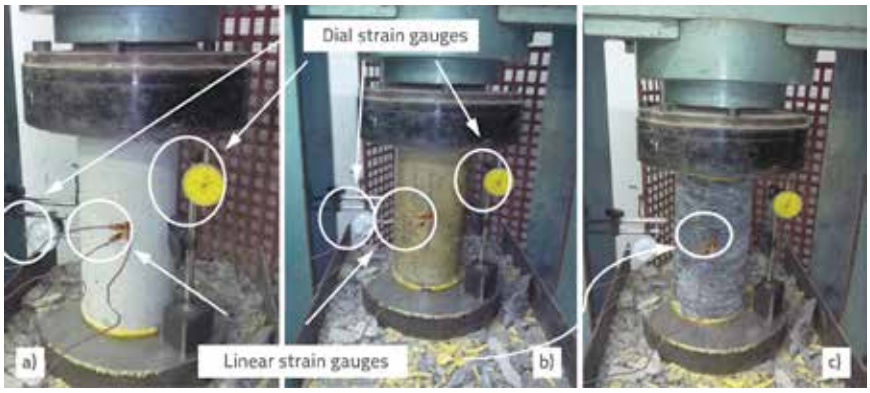

Figure 2. Test setup and arrangement for strain measurements: a) Control specimen; b) GFRP confined; c) CFRP confined

3. Test results and discussions

Tests were conducted on unconfined and confined concrete specimens to measure the compressive confined strength, and ultimate load carrying capacity, and to compare longitudinal, hoop and volumetric strains. The volumetric strain (ε_v) can be measured by adding the longitudinal strain (ε_l) and twice-hoop strain (ε_h).

$$\varepsilon_v = \varepsilon_l + 2\varepsilon_h$$

The comparison was carried out in terms of confined to unconfined strength, and gain in the axial load carrying capacity. Visual observations were also made during experiments and the results were analysed to determine behaviour of these specimens.

3.1. Axial compression tests

Axial compression tests were performed to determine the effect of FRP confinement for normal, medium and high strength concrete.

Table 3. Test data for axial compressive strength

Series of tests	Compressive strength of specimens [MPa]		
	Control	GFRP confined	CFRP confined
Series 1 (30 MPa)	29.79	38.13	47.37
	30.27	39.09	49.02
	29.03	38.13	46.82
Series 2 (42 MPa)	43.02	47.85	52.47
	42.54	47.92	52.75
	42.95	48.19	51.44
Series 3 (64 MPa)	64.88	68.87	74.46
	64.40	71.07	71.88
	64.74	70.67	70.84

Maximum strength, strain, and stiffness were measured through these tests on plain (control), GFRP, and CFRP confined concrete specimens. The axial compressive strength of control and FRP confined specimens is shown in Table 3. The results show that concrete specimens confined with CFRP exhibit a higher increase in axial compressive strength as compared to GFRP confined specimens, as shown in Figure 3. However, the confined strength increase decreases with an increase in the unconfined concrete strength. This

indicates that the strength of confined concrete depends on the type of confinement provided as well as on the original unconfined concrete strength. This effect of unconfined concrete on confinement has also been reported by Pessiki, Harries [11] in his study of FRP jacketed concrete.

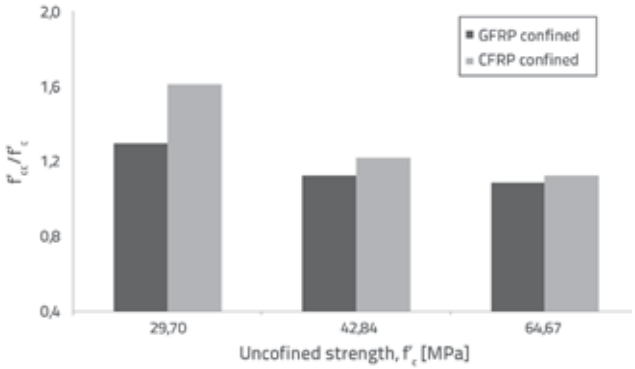

Figure 3. Comparison of GFRP and CFRP confined specimens with control specimens

3.2. Stress-strain response

The compressive tests conducted were also utilized on FRP confined concrete to study the stress-strain response. The stress-strain response of GFRP and CFRP confinement was also compared with previous studies. The comparison of stress-strain response of GFRP and CFRP confined specimens is presented in Figures 4, 5, and 6.

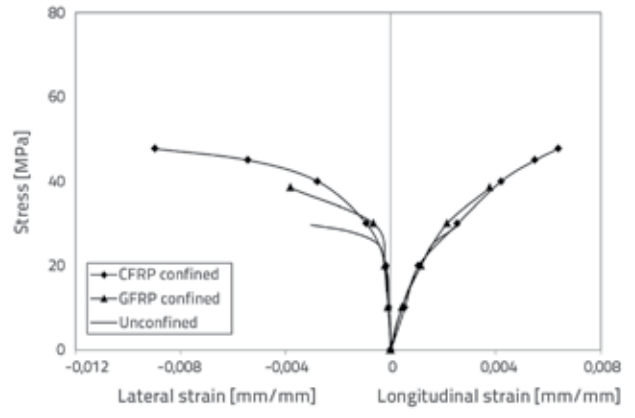

Figure 4. Stress-strain response of 30 MPa confined and unconfined concrete

The 30 MPa concrete shows a ductile behaviour as compared to other concrete types with lower stress values and higher strain values. For 42 MPa concrete specimens, CFRP confined specimens show increased enhancements in strength as well as ductility as compared to GFRP confined specimens. Conversely, the 64 MPa concrete exhibits a stiffer behaviour with higher stress values and lower corresponding strains in both longitudinal and hoop directions. The bifurcation point can be seen at longitudinal strain of 0.002 in the stress-strain response of all specimens. This is the point where the confining FRP layer starts to participate in assuming load. The CFRP confined specimens show higher enhancements in confinement and strength as compared to GFRP confined specimens. The CFRP confined specimens absorb more energy and show contraction under higher loading.

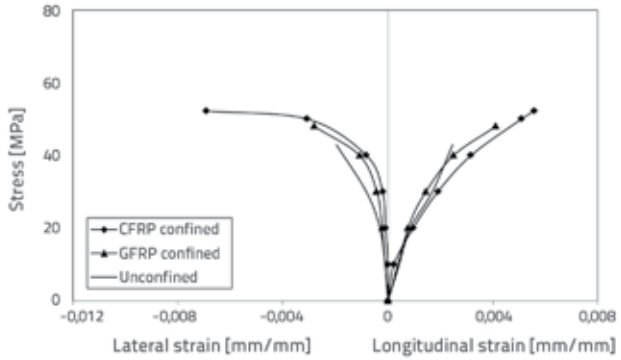

Figure 5. Stress-strain response of 42 MPa confined and unconfined concrete

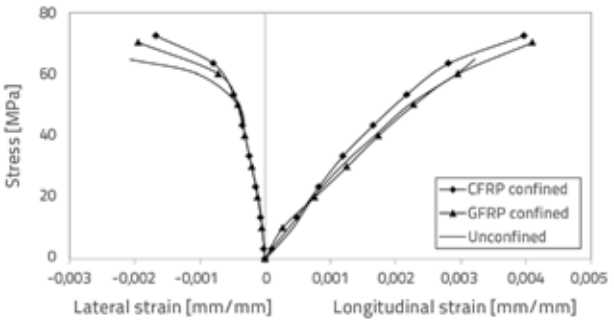

Figure 6. Stress-strain response of 64 MPa confined and unconfined concrete

The volumetric strain response for the three concrete types is shown in Figures 7, 8, and 9. The volumetric stress-strain response indicates that the specimens undergo contraction in longitudinal direction under axial compressive loading and then, just before failure, the specimens start expanding laterally exhibiting higher strain in lateral direction. The volumetric stress-strain response of GFRP confined specimens follows the pattern similar to that of unconfined specimens, where the specimens undergo contraction when subjected to axial compressive loading. GFRP confined specimens absorb energy up to their capacity and then start expanding in lateral direction but, due to confinement, the specimens absorb more energy compared to unconfined specimens. This can be explained by the fact that the confinement resists lateral expansion, which enables confined specimens to withstand higher loads before expanding.

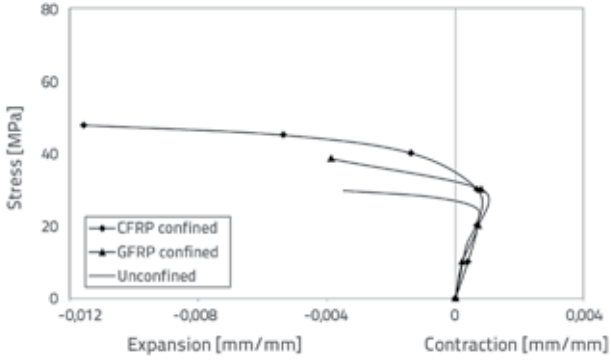

Figure 7. Volumetric strain response of 30 MPa confined and unconfined concrete.

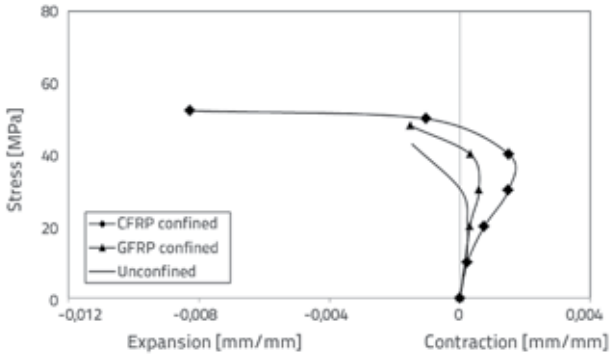

Figure 8. Volumetric strain response of 42 MPa confined and unconfined concrete

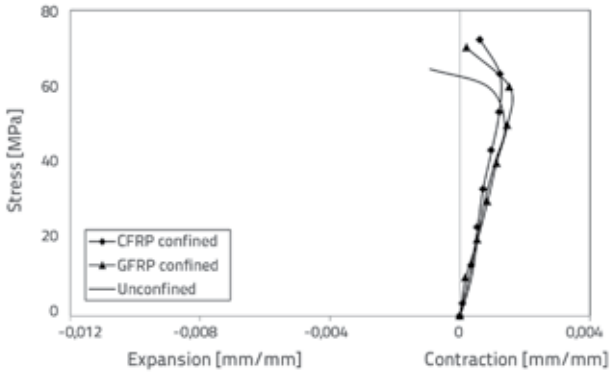

Figure 9. Volumetric strain response of 64 MPa confined and unconfined concrete

The CFRP confined concrete displays enhanced capacity to withstand load without much change in volume. The specimens resist both contraction and expansion as compared to GFRP confinement. The CFRP wrap takes part in absorbing energy along with concrete, resulting in more ductile behaviour as seen in 30 and 42 MPa concrete specimens, where the specimens fail at higher lateral strains. The behaviour of the 64 MPa concrete is more brittle owing to its higher strength as well as increased stiffness due to FRP. Therefore, FRPs show only an increased strength in HSC.

The test data is also compared to several previous works of this kind. Rahai and Sadeghian [8] used CFRP wraps measuring 0.9, 1.8, 2.7, and 3.6 mm in thickness and Bisby and Take [14] used CFRP wraps on 100 mm by 200 mm concrete cylinders to plot stress-strain response of confined concrete. Similarly Pessiki and Harries [11] used FRP wraps having different fibre strengths and densities on concrete specimens measuring 610 mm in height and 152 mm in diameter. The stress-strain response follows similar pattern as in the above studies. However, the values of corresponding stresses and strains are different, which is attributed to the difference in specimen size, fibre strength, and density of confining FRP wraps.

3.3. Stress and stiffness response of FRP confined concrete

The stress in the plain and wrapped concrete cylinder specimens was calculated by dividing the load applied with the original concrete cross sectional area. While calculating stress, the thickness of the wrap was not taken into account, as it is negligible as compared to the dimensions of the specimens. The stiffness was evaluated using the stress-strain response by calculating the slopes m_1 and m_2 at the bifurcation points as proposed by Samaan and Mirmiran [15]. The initial slope of the curve is m_1 and the slope after the bifurcation point is m_2, as shown in Figure 10.

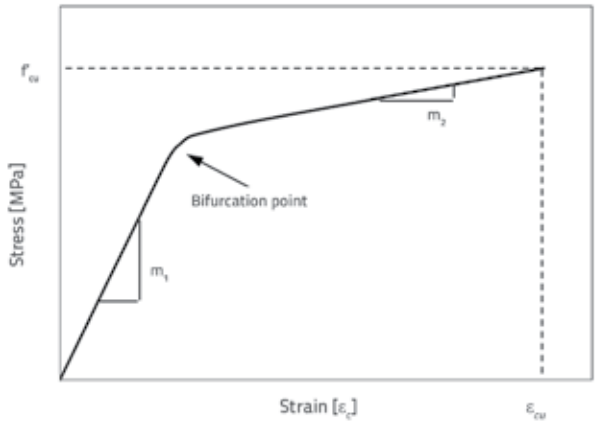

Figure 10. Stiffness slopes and bifurcation point of stress strain curve

The enhancement of stiffness is shown in Figure 11 where the ratio of stiffness of confined specimens (m'_1) to the stiffness of unconfined specimens (m_1) is plotted against the unconfined strength of specimens both in the axial and hoop directions.
With an increase in unconfined strength of concrete, the stiffness (m'_1) in longitudinal direction increases from 1.02 to 1.11 times in case of GFRP, and from 1.03 to 1.16 times in case of CFRP, as shown in Figure 11. The stiffness also increases in the hoop direction, but the increase in stiffness decreases as the unconfined strength of concrete increases. Only the 64 MPa concrete specimens show stiffer behaviour as compared to previous researches because of the difference in mix proportion

and test conditions whereas, on GFRP and CFRP confined concrete, the 30 MPa and 42 MPa specimens exhibit behaviour similar to the previously published one [8, 9].

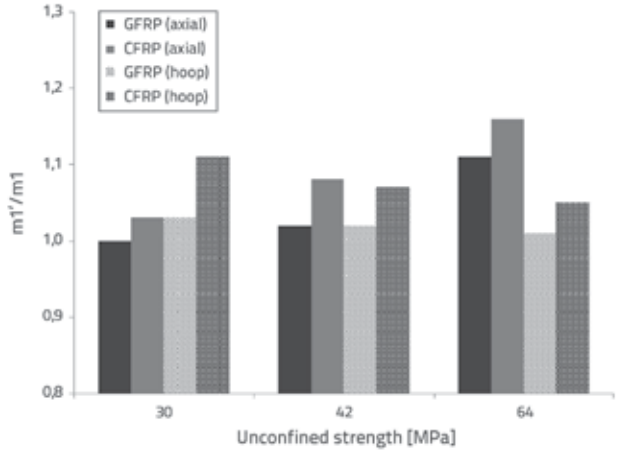

Figure 11. Comparison of stiffness of confined specimens

3.4. Strain response

The strain at specimen failure was recorded using strain gauges attached both in the vertical and horizontal directions and, hence, both the axial and hoop strain values were recorded. Maximum strain values are tabulated in Table 4.

Table 4. Average longitudinal and lateral strain at failure

Unconfined strength	Type of confinement	Average longitudinal strain at failure	Average lateral strain at failure
30 MPa	Unconfined	0.0026	0.0014
	GFRP wrapped	0.0045	0.0051
	CFRP wrapped	0.0064	0.0090
42 MPa	Unconfined	0.0029	0.0019
	GFRP wrapped	0.0041	0.0045
	CFRP wrapped	0.0056	0.0069
64 MPa	Unconfined	0.0032	0.0022
	GFRP wrapped	0.0041	0.0047
	CFRP wrapped	0.0052	0.0049

The ratio of failure strain of confined specimens (ε'_{cc}) to that of unconfined specimens (ε_c) is illustrated in Figure 12. It can be seen that hoop strains in unconfined plain concrete specimens are much lower compared to axial strains. The ratio between the lateral and longitudinal strains varies from 0.15 to 0.20 as the Poisson's ratio for concrete lies in this range. The increase in hoop strain of wrapped specimens was noted to be much higher than the axial strain increase because of the enhancement in ductility provided by FRP wrap confinement along the hoop direction. The CFRP confined specimens exhibit an increase of 5 times the strain of non-wrapped specimens, while GFRP wrapped specimens show an increase of up to 2 times the strain of unconfined specimens, which means that the CFRP confinement enhances the strain capacity in concrete much more as compared to GFRP confinement.

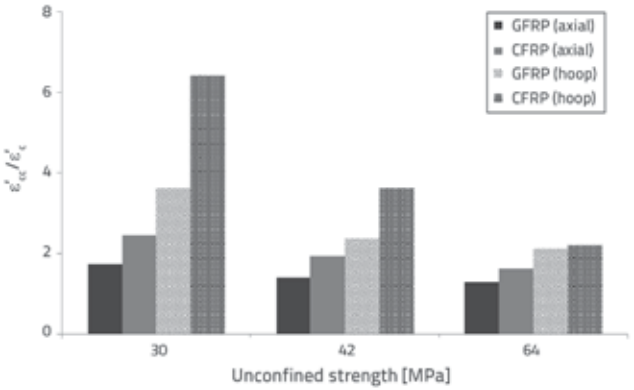

Figure 12. Comparison of axial and hoop strain of confined specimens

3.5. Ductility response

Ductility of a material is its ability to absorb energy. Ductile materials allow better stress distribution and give warning with regard to impending failure. In the case of FRP wrapped concrete specimens, specimen ductility is expressed in terms of deformability, which is defined as the ratio of energy absorption (or area under load-deflection curve) at ultimate strength to energy absorption at limiting curvature, as shown in the Figure 13.

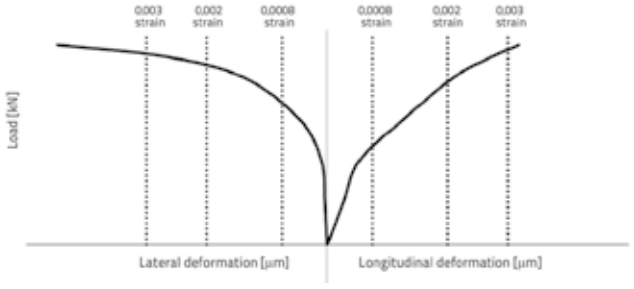

Figure 13. Load-deflection diagram with limiting strains to calculate energy absorption

In this study, deformability was calculated by finding the total energy under the curve up to failure and by calculating the ratio between the total energy and the energy at limiting strains of 0.0008, 0.002, and 0.003, as tabulated in Tables 5 and 6 for longitudinal and hoop directions, respectively.

Table 5. Deformability factors for unconfined, GFRP confined, and CFRP confined concrete specimens in longitudinal direction

Type of confinement	Limiting strains		
	0.0008	0.002	0.003
Unconfined	27.1742	0.1906	0.58
GFRP wrapped	43.5517	0.1868	0.46
CFRP wrapped	53.5423	0.1859	0.46

Table 6. Deformability factors for unconfined, GFRP confined, and CFRP confined concrete specimens in hoop direction

Type of confinement	Limiting strains		
	0.0008	0.002	0.003
Unconfined	17.5627	0.2332	0.59
GFRP wrapped	21.2005	0.2346	0.55
CFRP wrapped	32.1929	0.2380	0.55

Energy absorbed by confined specimens (Δ_{cc}) are compared in Figure 14 by considering the ratio of total energy absorbed by confined specimens to the total energy absorbed by unconfined specimens Δ_c. It can be seen in Figure 13 that energy absorbed by GFRP confined specimens is 1.33 to 1.99 times the energy absorbed by control specimens in longitudinal direction, whereas the energy absorbed in the hoop direction is 1.05 to 1.3 times the energy absorbed by unconfined concrete specimens. CFRP confined specimens show 1.34 to 2.87 times the energy absorbed by unconfined concrete specimens, while in the hoop direction this increment in energy absorption is 1.07 to 2.4 times. Moreover, as reported by Rahai and Sadeghian [8], the increment in energy absorption decreases as the unconfined strength of specimens increases in the longitudinal as well as in the hoop directions for both types of FRP confinements provided. It shows that the effectiveness of FRP confinement is more pronounced at lower strengths of concrete, and that it becomes less effective with an increase in concrete strength.

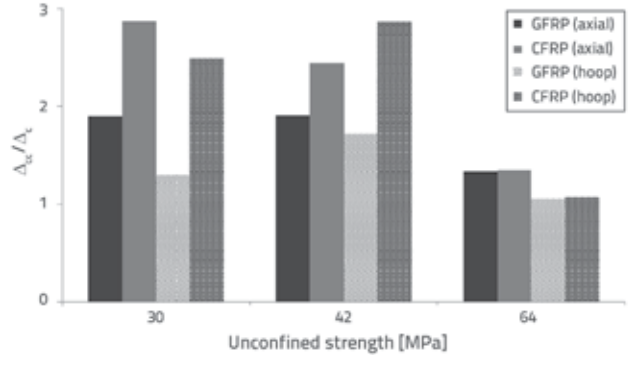

Figure 14. Comparison of energy absorption by confined specimens

3.6. Strength predictions of FRP confined concrete based on various codes and standards

Various design codes and guidelines have been developed for the prediction of confinement pressure, confined compressive strength, axial load carrying capacity, and other parameters. The most prominent design guidelines are those provided by American Concrete Institute ACI, Canadian Standards Association CSA, Canadian Intelligent Sensing for Innovative Structures ISIS, and European CEB/FIP Model Code that uses the guidelines provided in Technical Report by the *Fédération Internationale du Béton, fib Bulletin 14* [16-19]. Experimental results obtained in the test program are compared and correlated with theoretical values predicted in these FRP design guidelines and codes. Empirical formulae are shown in Table 7.

3.7. Comparison of theoretical guidelines with experimental results

Compressive strength values obtained through experimentation and theoretical guidelines are shown in Table 8. It can be noted that *fib* exact guidelines give the closest predictions for concrete confined with both FRP types. However, these guidelines overestimate the strength of CFRP confined specimens as the unconfined concrete strength increases from the domain of normal strength to high strength. The comparison of theoretical guidelines with experimental results is illustrated in Figures 15 and 16.

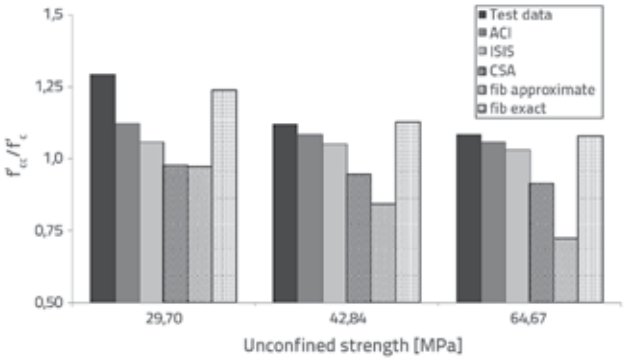

Figure 15. Comparison of test data and theoretical compressive strengths of GFRP

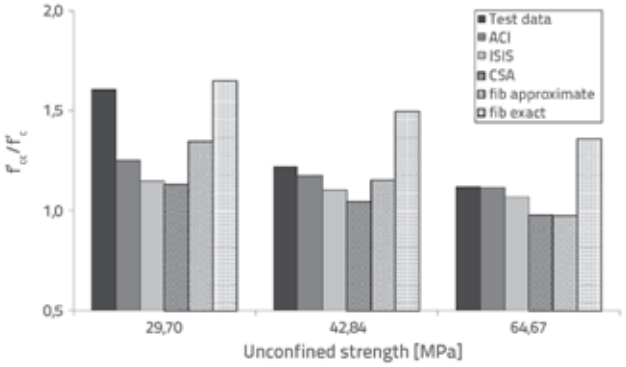

Figure 16. Comparison of test data and theoretical compressive strengths of CFRP

Table 7. Empirical formulae of design codes and standards

Design code	Confining pressure f_l [MPa]	Confined compressive strength of concrete f'_{cc} [MPa]	Ultimate axial strain ε_{ccu}	Ultimate load carrying capacity P_u [kN]
ACI-440-2R-2008	$f_l = \frac{2\varepsilon_{fe}E_f n t_f}{D}$ $f_l = \frac{2\varepsilon_{fe}E_f n t_f}{D}$	$f'_{cc} = f'_c + 3.3k_a\Psi_f f_l$ $f'_{cc} = f'_c + 3.3k_a\Psi_f f_l$	$\varepsilon'_{ccu} = \varepsilon'_c\left[1.5 + 12K_b\frac{f_l}{f'_c}\left(\frac{\varepsilon_{fe}}{\varepsilon'_c}\right)^{0.45}\right]$ $\varepsilon'_t = \frac{2f'_c}{E_c - E_2}$ $E_2 = \frac{f'_{cc} - f'_c}{\varepsilon'_{ccu}}$	$P_u = 0.85f'_{cc}(A_g - A_{st}) + f_y A_{st}$
CSA-S806-02	$f_l = \frac{2nt_f f_{frp}}{D}$ f_{frp} will be lesser of od 0.004 E_{frp} and 0.75* f_{frpu}	$f'_{cc} = 0.85f'_c + k_l k_s f_l$ $k_l = 6.7(f_l)^{-0.17}$		$P_u = \alpha f'_{cc}A_c + A_{st}f_y$ $\alpha = 0.85\text{-}0.0015f'_c$
ISIS M04 2001	$f_l \geq 4$ MPa	$f'_{cc} = f'_c(1 + \alpha_{pr}\omega_w)$ $\omega_w = \frac{f_l}{f'_c}$		$P_u = \alpha f'_{cc}A_c + A_{st}f_y$ $\alpha = 0.85\text{-}0.0015f'_c$
CEB/FIP Model Code 2010 fib Approx Method	$f_l = \frac{2N_b f_{frpu} t_{frp}}{D_g}$ For full wrapped circular sections $\rho_f = \frac{4nt_f}{10}\left(\frac{b_f}{s}\right)$	$f'_{cc} = f'_c(0.2 + 3\sqrt{\frac{f_l}{f'_c}})$		$P_u = \lambda n f'_{cc}A_c + A_{st}f_y$ $\lambda = 0.8$
CEB/FIP Model Code 2010 fib Exact Method		$f_{cu} = \varepsilon_{cu}E_{sec.u}$ $E_{sec,u} = \frac{E_c}{1 + 2\beta\varepsilon_{fu}}$ $E_c = 4730\sqrt{f'_c}$	$\varepsilon_{cu} = \varepsilon_{cc}\left[\frac{E_{cc}(E_c - E_{sec,u})}{E_{sec,u}(E_c - E_{cc})}\right]^{1-\frac{E_{cc}}{E_c}}$ $E_{cc} = \frac{f_{cc}}{\varepsilon_{cc}}$	$P_u = \lambda f'_{cc}A_c + A_{st}f_y$ $\lambda = 0.8$

Notation list

P_u - Axial load carrying capacity
f'_{cc} - Compressive strength of confined concrete
A_g - Cross sectional area of the confined concrete
A_{st} - Longitudinal reinforcing steel area
f_y - Yield strength of longitudinal bars
f'_c - Unconfined concrete compressive strength
f_l - Lateral confinement pressure
n - Number of FRP layers
t_f - Thickness of FRP layer
E_f - FRP modulus of elasticity
ε_{fe} - FRP effective strain = k_e
Ψ_f - FRP strength reduction factor = 0.95
N_b - Number of layers of FRP
f_{frpu} - Ultimate strength of FRP
t_{frp} - Thickness per layer of FRP
D_g - Diameter of the member
b_f - Width of FRP strip in partial wrapping
s - Pitch in partial wrapping
k_e - Confinement effectiveness coefficient = 0.55
λ - Strength reduction factor = 0.8
E_{secu} - Secant modulus of elasticity
ρ_f - Volumetric ratio of FRP reinforcement
$\rho_f = \frac{4nt_f}{10}\left(\frac{b_f}{s}\right)$ - for circular sections

Table 8. Experimental and theoretical data for confined and unconfined compressive strength

Unconfined strengths f'_c [MPa]	Confinement	Experimental f'_{cc} [MPa]	ACI f'_{cc} [MPa]	CSA f'_{cc} [MPa]	ISIS f'_{cc} [MPa]	fib approx f'_{cc} [MPa]	fib exact f'_{cc} [MPa]
29.7	GFRP	38.45	33.34	29.7	31.38	28.89	36.82
42.84		47.99	46.48	42.84	44.95	36.13	48.37
64.67		70.20	68.32	64.67	66.78	46.79	69.84
29.7	CFRP	47.74	37.19	33.61	34.16	40.03	48.99
42.84		52.22	50.33	44.78	47.3	49.51	64.11
64.67		72.39	72.16	64.67	69.13	63.24	87.98

Table 9. Experimental and theoretical data for ultimate load carrying capacity of confined and unconfined specimens

Unconfined strengths [MPa]	Confinement	Experimental P_u [kN]	ACI P_u [kN]	CSA P_u [kN]	ISIS P_u [kN]	fib approx P_u [kN]	fib exact P_u [kN]
29.7	GFRP	699.79	517	430.6	456	420.63	536.09
42.84		873.36	720.7	605.87	635.74	526.02	704.26
64.67		1277.70	1059.2	876.53	905.13	681.34	1016.87
29.7	CFRP	868.81	576.6	493	495.25	584.16	713.3
42.84		950.40	780.38	641.83	669	720.96	933.44
64.67		1317.56	1177	876.53	937	920.85	1280.93

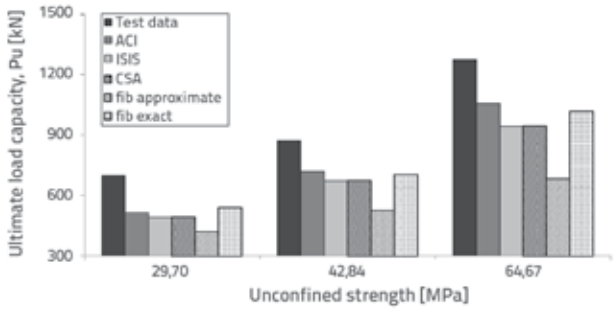

Figure 17. Comparison of test data and theoretical ultimate load carrying capacities of GFRP

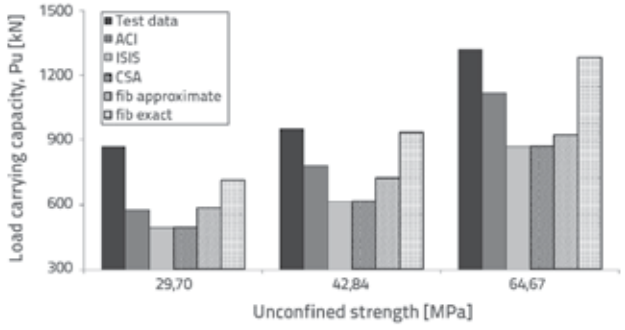

Figure 18. Comparison of test data and theoretical ultimate load carrying capacities of CFRP

Though more conservative than *fib*, ACI gives exact guidelines, and closer predictions at higher strengths of unconfined concrete. *fib* approximate guidelines and CSA guidelines give highly conservative predictions to such extent that the predicted values cannot be safely used based on these guidelines. This can be attributed to the fact that *fib* approximate guidelines were developed for FRP that can provide high confining pressure and CSA uses a factor of 0.85 for the reduction of unconfined concrete strength.

The values of ultimate load carrying capacity from experimentation and predictions of FRP design guidelines are shown in Table 9, while their comparison is illustrated in Figures 17 and 18. It can be observed that all the guidelines considered give significantly conservative predictions for lower concrete strengths, but the predictions get closer to actual results at higher strengths of unconfined concrete. The *fib* exact method gives the closest predictions of CFRP as compared to other FRP confined concrete design guidelines. ACI guidelines predict better results as compared to the *fib* exact method in the case of GFRP confinement. Among all the guidelines, the *fib* approximate method gives the most conservative results in the case of GFRP confinement, while CSA gives the most conservative results in the case of CFRP confinement, as confirmed in another comparative study of these models [20].

3.8. Failure modes and patterns

The surface of wrapped cylinder specimens was carefully observed after the achievement of failure loads. Failure modes of specimens wrapped with GFRP and CFRP are shown in Figure 19. All CFRP-wrapped specimens failed by the FRP wrap rupture due to hoop tension. Similar case was observed for GFRP wrapped specimens. The collapse occurred almost without any advance warning by sudden rupture of the composite wrap. For all confined specimens, delamination was not observed at the overlap location of the jacket.

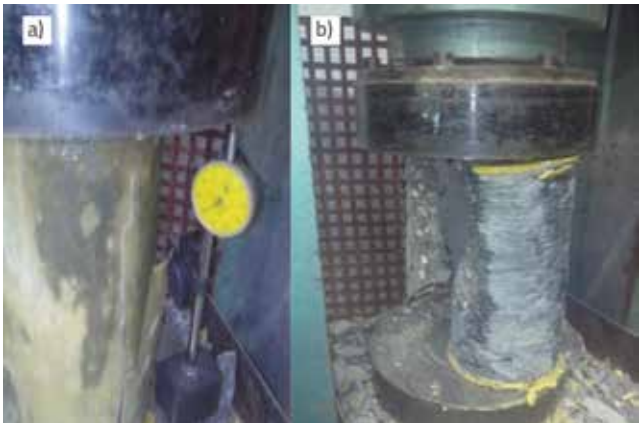

Figure 19. Failure modes and patterns of tested specimens: a) GPRF confined; b) CFRP confined

4. Conclusions

Based on the research presented in this paper, the following conclusions can be made:

- The axial compressive strength of concrete specimens increases if they are confined with FRPs. Specimens wrapped with CFRP reveal greater improvement in confined compressive strength

from 12 to 61 %, whereas GFRP confined specimens show 9 to 29% increase in compressive strength.
- The effectiveness of FRP confinement decreases with an increase in unconfined strength of substrate concrete.
- The increase of longitudinal (axial) strain in the CFRP confined concrete is by 1.99 to 2.22 times higher compared to the GFRP confined concrete, whereas the hoop strain in the CFRP confined concrete is by 1.08 to 2.04 times higher than that of the GFRP confined concrete in case of 30 to 64 MPa unconfined concrete strengths. Both FRP confinements enhance the hoop strain far more than longitudinal strain, but this enhancement effect decreases with an increase in the unconfined strength of concrete.
- Stiffness of the FRP confined concrete is also affected by unconfined strength of concrete as it decreases with an increase in unconfined concrete strength and vice versa.
- The increase in total energy absorption is more pronounced in the CFRP confined concrete as compared to GFRP confined concrete; however, this increment in total energy absorption decreases with an increase in the unconfined strength of concrete.
- The American Concrete Institute ACI 440.2R 2008, the Canadian Standard Association (CSA- S806 02), Intelligent Sensing for Innovative Structures Canada (ISIS M04 2001), and *fib* approximate method guidelines, show conservative predictions of confined compressive strength of concrete. However, predictions given in these guidelines give closer confined strength results with an increase in the unconfined strength of concrete.
- Compared to other FRP design codes and guidelines, *fib* exact guidelines give the closest predictions for both FRPs; however, they overestimate strength of the CFRP confined concrete with an increase in the unconfined strength of concrete.
- ACI 440.2R 2008 gives conservative results as compared to *fib* exact guidelines and is less affected by strength of unconfined concrete.
- CSA-S806-02 guidelines show the most conservative results. This is attributed to the safety factor of 0.85 used by CSA-S806-02 for reduction of the unconfined concrete strength, which leads to underestimation of the effectiveness of CFRP.
- For GFRP confinement, CSA-S806-02 and *fib* approximate guidelines give lower strength of confined specimens compared to unconfined specimens.

Acknowledgments

The research presented in this paper was supported by National University of Sciences and Technology, Islamabad, Pakistan. Any opinion, finding and conclusion explained in this paper can be attributed solely to the authors and does not necessarily reflect the views of the sponsors.

REFERENCES

[1] Seible, F., Priestley, M.J.N., Hegemier, G.A., Innamorato, D.: Seismic retrofit of RC columns with continuous carbon fiber jackets. Journal of composites for Construction, 1 (1997) 2, pp. 52-62.

[2] Khaliq, W.: Performance characterization of high performance concretes under fire conditions, in PhD Dissertation, Michigan State University, East Lansing, MI. pp. 345, 2012.

[3] Khaliq, W., Kodur, V.: Thermal and mechanical properties of fiber reinforced high performance self-consolidating concrete at elevated temperatures, Cement and Concrete Research, 41 (2011) 11, pp. 1112-1122.

[4] Ozbakkaloglu, T.: Axial compressive behavior of square and rectangular high-strength concrete-filled FRP tubes, Journal of composites for Construction, 17 (2012) 1, pp. 151-161.

[5] Mirmiran, A., Shahawy, M., Samaan, M., El Echary, H., Mastrapa, J.C., Pico, O.: Effect of column parameters on FRP-confined concrete, Journal of composites for Construction, 2 (1998) 4, pp. 175-185.

[6] Wu, G., Lü, Z., Wu, Z.: Strength and ductility of concrete cylinders confined with FRP composites, Construction and Building Materials, 20 (2006) 3, pp. 134-148.

[7] Nanni, A., Bradford, N.M.: FRP jacketed concrete under uniaxial compression, Construction and Building Materials, 9 (1995) 2, pp. 115-124.

[8] Rahai, A., Sadeghian, PP., Ehsani, M.: Experimental Behavior of Concrete Cylinders Confined with CFRP Composites, The 14th World Conference on Earthquake Engineering, 2008.

[9] Li, G.: Experimental study of FRP confined concrete cylinders. Engineering structures, 28 (2006) 7, pp. 1001-1008.

[10] Parvin, A., Jamwal, A.S.: Effects of wrap thickness and ply configuration on composite-confined concrete cylinders, Composite structures, 67 (2005) 4, pp. 437-442.

[11] Pessiki, S., Harries, K.A., Kestner, J.T., Sause, R., Ricles, J.M.: Axial behavior of reinforced concrete columns confined with FRP jackets, Journal of composites for Construction, 5 (2001) 4, pp. 237-245.

[12] Rochette, P.P., Labossiere, P.P.: Axial testing of rectangular column models confined with composites. Journal of composites for Construction, 4 (2000) 3, pp. 129-136.

[13] Thériault, M., Neale, K.W., Claude, S.: Fiber-reinforced polymer-confined circular concrete columns: investigation of size and slenderness effects, Journal of composites for Construction, 8 (2004) 4, pp. 323-331.

[14] Bisby, L., Take, W.A., Caspary, A.: Effects of Unconfined Concrete Strength on FRP Confinement of Concrete, International Institute for FRP in Construction, 2007.

[15] Samaan, M., Mirmiran, A., Shahawy, M.: Model of concrete confined by fiber composites, Journal of Structural Engineering, 124 (1998) 9, pp. 1025-1031.

[16] ACI 440.2: Guide for the design and construction of externally bonded FRP systems for strengthening concrete structures, American Concrete Institute, Farmington Hills, USA, 2002.

[17] CSA S806-02: Design and construction of building components with fibre-reinforced polymers, Canadian Standards Association, 2002.

[18] ISIS M04-01: Externally Bonded FRP for Strengthening Reinforced Concrete Structures, The Canadian Network of Centres of Excellence on Intelligent Sensing for Innovative Structures, Winnipeg, MB, Canada, 2001.

[19] fib, Fédération internationale du Béton: Externally bonded FRP reinforcement for RC structures, Bulletin No. 14, Technical Report2001, Lausanne, Switzerland.

[20] Chaallal, O., Hassan, M., LeBlanc, M.: Circular columns confined with FRP: Experimental versus predictions of models and guidelines, Journal of composites for Construction, 10 (2006) 1, pp. 4-12.